Remote Sens. **2012**, *4*, 3364-3389; doi:10.3390/rs4113364

OPEN ACCESS

Remote Sensing

ISSN 2072-4292

www.mdpi.com/journal/remotesensing

Article

How Normalized Difference Vegetation Index (NDVI) Trends from Advanced Very High Resolution Radiometer (AVHRR) and Système Probatoire d'Observation de la Terre VEGETATION (SPOT VGT) Time Series Differ in Agricultural Areas: An Inner Mongolian Case Study

He Yin [1,*], Thomas Udelhoven [2], Rasmus Fensholt [3], Dirk Pflugmacher [1] and Patrick Hostert [1]

[1] Geography Department, Humboldt-Universität zu Berlin, Unter den Linden 6, D-10099 Berlin, Germany; E-Mails: dirk.pflugmacher@geo.hu-berlin.de (D.P.); patrick.hostert@geo.hu-berlin.de (P.H.)

[2] Environmental Remote Sensing and Geoinformatics Department, University of Trier, Behringstr. 15, D-54286 Trier, Germany; E-Mail: udelhove@uni-trier.de

[3] Department of Geography and Geology, University of Copenhagen, Øster Voldgade 10, DK-1350 Copenhagen, Denmark; E-Mail: Rf@geo.ku.dk

* Author to whom correspondence should be addressed; E-Mail: he.yin@geo.hu-berlin.de; Tel.: +49-30-2093-9341; Fax: +49-30-2093-6848.

Received: 31 August 2012; in revised form: 24 October 2012/ Accepted: 31 October 2012 / Published: 6 November 2012

Abstract: Detailed information from global remote sensing has greatly advanced our understanding of Earth as a system in general and of agricultural processes in particular. Vegetation monitoring with global remote sensing systems over long time periods is critical to gain a better understanding of processes related to agricultural change over long time periods. This specifically relates to sub-humid to semi-arid ecosystems, where agricultural change in grazing lands can only be detected based on long time series. By integrating data from different sensors it is theoretically possible to construct NDVI time series back to the early 1980s. However, such integration is hampered by uncertainties in the comparability between different sensor products. To be able to rely on vegetation trends derived from integrated time series it is therefore crucial to investigate whether vegetation trends derived from NDVI and phenological parameters are consistent across products. In this paper we analyzed several indicators of vegetation change for a range of agricultural systems in Inner Mongolia, China, and compared the results across different satellite archives. Specifically, we compared two of the prime NDVI archives—AVHRR

Global Inventory Modeling and Mapping Studies (GIMMS) and SPOT Vegetation (VGT) NDVI. Because a true accuracy assessment of long time series is not possible, we further compared SPOT VGT NDVI with NDVI from MODIS Terra as a benchmark. We found high similarities in interannual trends, and also in trends of the seasonal amplitude and integral between SPOT VGT and MODIS Terra ($r > 0.9$). However, we observed considerable disagreements in NDVI-derived trends between AVHRR GIMMS and SPOT VGT. We detected similar discrepancies for trends based on phenological parameters, such as amplitude and integral of NDVI curves corresponding to seasonal vegetation cycles. Inconsistencies were partially related to land cover and vegetation density. Different pre-processing schemes and the coarser spatial resolution of AVHRR GIMMS introduced further uncertainties. Our results corroborate findings from other studies that vegetation trends derived from AVHRR GIMMS data not always reflect true vegetation changes. A more thorough understanding of the factors introducing uncertainties in AVHRR GIMMS time series is needed, and we caution against using AVHRR GIMMS data in regional studies without applying regional sensitivity analyses.

Keywords: NDVI; trend analysis; AVHRR GIMMS; SPOT VGT; MODIS Terra; Inner Mongolia; agriculture

1. Introduction

Remote sensing data have provided unique insights for global environmental change research during the past decades [1–3]. Global data archives such as those based on imagery acquired by the Moderate-Resolution Imaging Spectroradiometer (MODIS), Système Probatoire d'Observation de la Terre VEGETATION (SPOT VGT) or the National Oceanic and Atmospheric Administration (NOAA) Advanced Very High Resolution Radiometer (AVHRR) are key to understanding ecosystem changes from regional to global scales [4–8]. Without detailed information from global remote sensing systems, global environmental change research would be hampered from understanding Earth as a system [9–11].

Monitoring agricultural change trajectories over long time periods is critical to gain a better understanding of the Earth System's carrying capacities [12–14]. Gradual or long-term change processes, such as ecosystem degradation due to agricultural over-use, can only be detected and characterized with confidence from time series. However, extracting trends from time series can be challenging due to short-term (e.g., phenological) variations in the data or overall low signal-to-noise-ratios [15–18]. It is hence necessary to establish long enough time series to reliably capture vegetation trends in agricultural ecosystems [19–21]. In this paper, we strive to better understand how time series from global satellite archives compare across one of China's prime agricultural areas and how trends derived from time series relate to agricultural change.

Among the various remote sensing-based vegetation measures utilized in agricultural monitoring, the Normalized Difference Vegetation Index (NDVI) is the most widely used proxy for vegetation cover and production [22–26]. There is a strong relationship between NDVI and agricultural yield [27,28]. Vegetation properties, such as length of growing season, onset date of greenness, and

date of maximum photosynthetic activity are often derived from NDVI time series for monitoring changes in agricultural systems [29–32]. These phenological indicators emphasize different characteristics of terrestrial ecosystems to gain a better understanding of structure and function of land cover and associated changes [7,33,34]. Phenology, *i.e.*, the timing of recurring life cycle events, may for example shift in response to natural or anthropogenic disturbances in agricultural ecosystems [35,36]. Environmental scientists have an increasing interest in spatially explicit phenological data to better understand agricultural change processes associated with land use and climate change. In this context, remote sensing-based time series of NDVI are increasingly used to obtain phenological data at regional to global scales [37–40].

Daily NDVI series of global coverage derived from AVHRR data have been extensively used for land change research, including agricultural ecosystems [2,29,41–44]. Because AVHRR was originally designed for deriving information about the Earth's atmosphere, its radiometric and spatial resolution is not optimized for vegetation monitoring [45,46]. Nevertheless, the AVHRR systems are the only available instruments that have provided repeated, long-term observations of global vegetation properties in an operational mode since June 1979, the launch of NOAA-6.

Since the late 1990s, satellite missions have tremendously improved monitoring capabilities and data quality, specifically with regard to data calibration and standardized pre-processing schemes. Among others, bandwidths and spectral response in the red and near-infrared bands needed for NDVI calculation have been improved compared to AVHRR [47,48]. While newer remote sensing instruments such as SPOT-VEGETATION and MODIS supply higher quality data, their relatively short service record compared to AVHRR has been a limiting factor for analyzing long-term surface conditions. Therefore, AVHRR remains an invaluable and irreplaceable archive of historical land surface information when targeting long-term change processes in ecosystem analysis, such as agricultural expansion and intensification [49–51].

Despite the need for integrating NDVI time series from different sensors, it is not well understood how phenological parameters and change trends derived from NDVI time series compare across sensors in different regions. Little information exists on which factors might lead to systematic biases, specifically in areas with low and strongly varying NDVI [52]. With the advent of new generations of sensors, [8], for example, pointed out that differences between AVHRR and MODIS time series in the spectral, radiometric, and spatial domain need to be better understood to meet the needs of long-term agricultural change research. In general, it is crucial to better understand differences in time series products from different NDVI archives acquired from, among others, NOAA AVHRR, SPOT VGT and MODIS [53–55].

There have been several studies showing a generally acceptable agreement between NDVI time series from AVHRR sensors and MODIS, MERIS (MEdium Resolution Imaging Spectrometer), or SPOT VGT. [56] examined NDVI time series between 2002 and 2003 derived from AVHRR (NOAA-16 and NOAA-17) and MODIS (MOD13A2; Collection 4), and found good linear relationships for 89% of the NDVI values for the conterminous United States. Swinnen *et al*. [57] found a good linear agreement between the SPOT-VGT 10-day synthesis product (S10) and the AVHRR Local Area Coverage (LAC) Level 1b datasets after conducting sensor calibrations to improve consistency for Southern Africa.

However, these studies were based on correlation analyses, which mainly proof the coherence of the seasonal, sinusoidal-like NDVI patterns. As phenological changes are often much greater than long-term

vegetation trends, these analyses are not sensitive enough to allow inferences on long-term vegetation trends. Less research has focused on directly comparing trends derived from different NDVI datasets. For regional and global agriculture monitoring, however, it is crucial to know whether trends derived from different NDVI archives are comparable or not. Using four NDVI time series derived from AVHRR spanning 1982 to 1999, Alcaraz-Segura *et al*. [52] evaluated the differences in spatial patterns of trends in Pathfinder (PAL), Fourier-Adjustment, Solar zenith angle corrected, Interpolated Reconstructed (FASIR), GIMMS, and Land Long Term Data Record (LTDR) datasets. They found that GIMMS-derived trends differed the most and concluded that it is necessary to compare trends from different AVHRR-based NDVI products with those derived from other sensors. One study focusing on the comparability of NDVI-based trend derivatives from AVHRR, MODIS and SPOT VGT data was performed by [5] for the Sahel region. They concluded that GIMMS, MODIS 16-day NDVI and SPOT VGT 10-day composites produced largely similar trends, with variations increasing towards more humid climate regimes, *i.e.*, higher biomass. Song *et al*. [58] examined correlation and compared trend maps from AVHRR GIMMS and SPOT VGT visually across China from 1999 to 2006, they concluded that these two products correlated well and trends are largely coherent, apart from desert areas. A global comparison between the newly-processed GIMMS3g archive and MODIS data showed that global class-wise trends across biomes exhibit similar tendencies, but spatial patterns at the local to regional scale do often correlate less well [59].

Findings on the comparability of vegetation trends derived from different satellite data archives are inconclusive and not available across the full range of biomes. While the AVHRR GIMMS dataset has been cross-calibrated with data from other sensors [51], a deeper knowledge on the compatibility of vegetation trends derived from these cross-calibrated data is needed across a range of different agricultural systems.

We chose Inner Mongolia as a test region, which allowed us to compare NDVI-based trends from different sensors across a climatic gradient from sub-humid to arid environments. While agricultural intensification in Inner Mongolia started in the late 1970s, policies to protect the environment were mostly implemented since the late 1990s, *i.e.*, related effects will only be detectable in recent data. Such long time periods of agricultural change require a coupling of different NDVI archives in a consistent framework to capture the full range of change processes. The aim of this paper is a comprehensive comparison of vegetation trends in various agricultural systems derived from AVHRR GIMMS and SPOT VGT NDVI archives, using MODIS as a benchmark for SPOT VGT. We strive to better understand how consistent indicators of vegetation change are between these archives. We therefore ultimately pose the question which restrictions apply when analyzing long-term trends from joint NDVI archives for agricultural areas.

2. Materials

2.1. Study Area

Our study area is located in central and western Inner Mongolia (Figure 1). The region is characterized by an arid to sub-humid climate with a strong zonal distribution of rainfall and vegetation from East to West [31,60]. Along with the zonal precipitation patterns, land uses follow a

distinct gradient. The northeastern part of the study area is dominated by deciduous forest and in the lowlands by agriculture. Between the forested East and the desert in the West, land cover is dominated by various grassland ecosystems.

We selected the Hinggan region in densely-vegetated northeast Inner Mongolia and the sparsely vegetated Ordos region as two prototypic landscapes for testing our analysis scheme and for an in-depth evaluation of results. Hinggan is known as an ecological transition zone, with landscapes ranging from cultivated cropland in the eastern plain to forests in the mountainous West. Ordos is dominated by dry grasslands, desert and irrigated cropland along the Yellow River [61,62].

Figure 1. Mean annual rainfall (1999–2006) in Inner Mongolia interpolated from China Meteorological Administration (CMA) data (**A**). Elevation data from Shuttle Radar Topography Mission (SRTM) digital elevation model (**B**). Reclassified land cover map of Inner Mongolia as provided by the Chinese Academy of Science (CAS) [72] for the year 2000. Black frames showing focus regions. Inset showing Inner Mongolia in Asia (**C**).

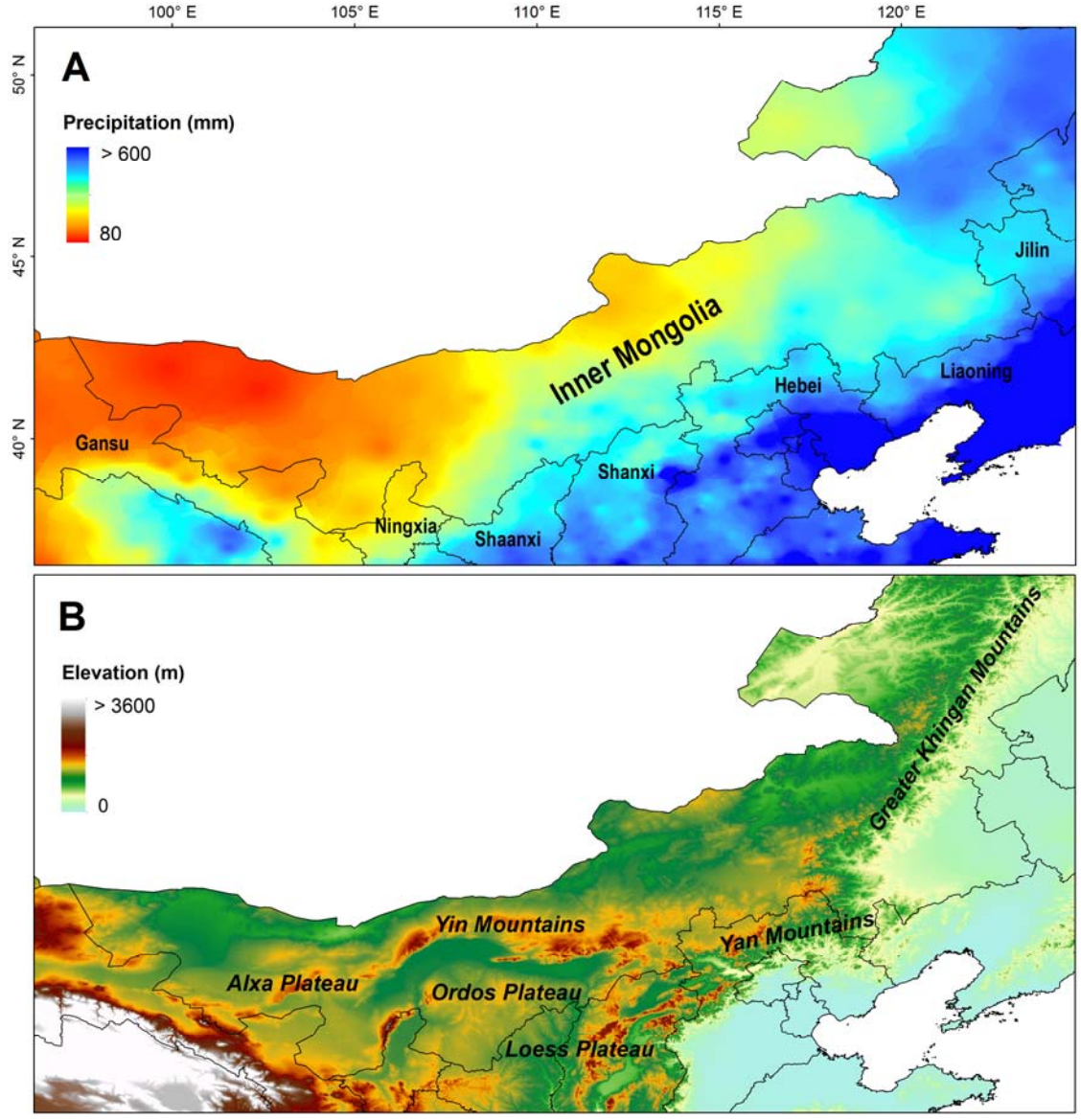

Figure 1. *Cont.*

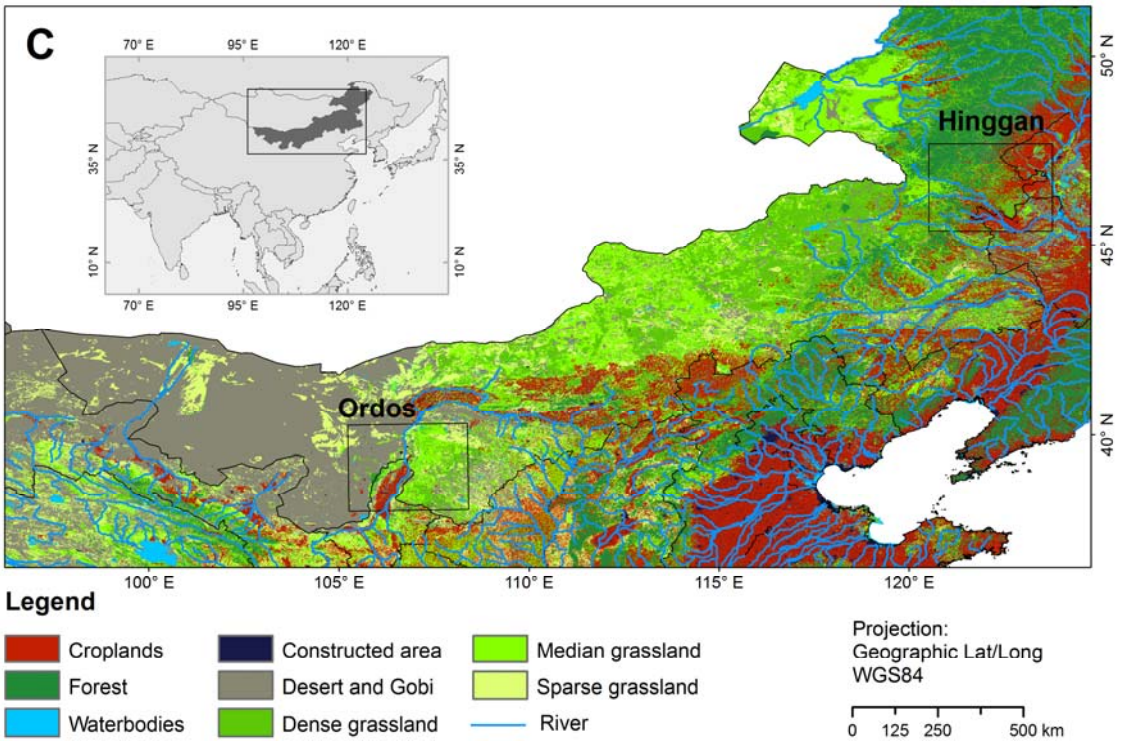

Considering agricultural change during the last decades, Inner Mongolia has undergone several land use transitions. Those changes are on the one hand triggered by a tremendously increasing demand for agricultural products in China [63,64], and on the other hand by the need to stop ongoing land degradation [49,65]. In Inner Mongolia, four different change processes can be distinguished on agricultural land: First, the semi-arid to sub-humid grasslands of the steppe regions have been and still are intensively grazed. Extended areas heavily degraded over time, which enforced restrictive grassland exclosure policies [50,66,67]. Second, in the more humid regions of Inner Mongolia intensive cropping systems developed. These also prevail along the river valleys of the semi-arid areas of Inner Mongolia, where irrigation systems allow for higher yields and more water-demanding crop species. This trend is still ongoing [68,69]. Third, agricultural land on slopes has been affected by China's Sloping Land Conversion Program, also referred to as the national "Grain for Green" Program [70,71]. In mountainous terrain we consequently expect a greening up of previously cropped areas. Fourth, natural forest protection and afforestation in croplands as wind shelter is extensively practiced in Inner Mongolia to combat land degradation and prevent sand storms, known as the "Green Great Wall" and "The Combating Desertification Program in Wind-Sand Source Areas Affecting Beijing and Tianjin" initiatives [68,69]. Almost all the croplands in the study region are covered by these programs, while the exact time of implementation depends on local policies and may accordingly vary.

2.2. Data

2.2.1. AVHRR NDVI Composites

The AVHRR NDVI archive employed in this study was obtained from the NASA GIMMS group [73] and covered the years 1999 to 2006. We selected AVHRR GIMMS because it is the only

updated archive and also the most widely used global AVHRR dataset [51]. GIMMS data are 15-day maximum value composites (MVC) at 8-km spatial resolution produced from Global Area Coverage (GAC) 1B data [51]. Data from six AVHRR instruments on different satellite platforms were used to produce this dataset. To ensure the continuity of NDVI time series derived from different instruments, GIMMS data have undergone rigorous data post-processing, including corrections of residual differences between sensors, viewing geometry caused by orbit drift, volcanic aerosols effects, and low signal-to-noise ratios due to sub-pixel cloud contamination [51]. Furthermore, Empirical Mode Decomposition (EMD) has been employed to identify and remove components of the NDVI signal that are largely related to the satellite drift on the Solar Zenith Angle (SZA) [74,75]. Finally, temporally overlapping SPOT Vegetation NDVI time series were used to intercalibrate the NOAA-14 and NOAA-16 NDVI time series [75]. To this end, non-linear regression was performed to establish coefficients that transform historical data into the same value range as that of MODIS and SPOT [51,76].

2.2.2. SPOT-VGT NDVI Composites

The SPOT-VGT S10 products obtained from the Vlaamse Instelling voor Technologisch Onderzock (VITO) Image Processing center (http://free.vgt.vito.be/) are derived from SPOT-VGT P (P = physical) products. Launched on 24 March 1998, the VGT 1 on board SPOT-4 began capturing data until February 2003, when VGT 2 on board SPOT-5 became the nominal instrument. The VEGETATION instrument has several advantages compared to AVHRR, including better navigation, improved radiometric sensitivity, reduced geometric distortions, and 4 spectral bands instead of 2 in the visible to near infrared (VISNIR) spectral domain [77]. The SPOT-VGT S10 products are compiled by merging segments (data strips) acquired in a 10-day MVC at 1-km spatial resolution based on VGT-P products, which have been atmospherically corrected for molecular and aerosol scattering, water vapor, ozone and other gas absorptions [78]. A slight increase in NDVI after 2003 has been reported due to differences in radiometric calibration methods and band widths between VGT 1 and VGT 2. The observed 3.5% increase in NDVI (for values > 0.3 only) is related to a bias in the near-infrared and red band of 6.3% and 2.1%, respectively [5,78,79].

2.2.3. MODIS Terra NDVI Composites

We obtained MODIS-based NDVI data between 2001 and 2010 from the MODIS-Terra Vegetation Index (VI) products (MOD13Q1, Collection 5). We acquired the data from the United States Geological Survey (USGS) Land Processes (LP) Distributed Active Archive Center (DAAC) at the Earth Resources Observation and Science (EROS) Data Center. The MODIS VI archive is available at a nominal 250-m spatial resolution and composited with a time interval of 16-days. Unlike AVHRR GIMMS and SPOT-VGT products, which use the simpler MVC method for compositing, MODIS VI products use a more sophisticated compositing algorithm that consists of two components: (1) a bidirectional reflectance distribution function composite (BRDF-C), and (2) a constrained view angle-maximum value composite (CV-MVC). These algorithms were designed to constrain the strong angular variations encountered in the MVC method and to reduce spatial and temporal discontinuities in the composited product [47]. The MODIS VI archives have shown a better ability to provide useful

radiometric and biophysical information for land surface characterization than previously available NOAA-AVHRR datasets [47,80].

2.2.4. Other Data

The Chinese Academy of Sciences' Land-Use/Land-Cover Change (LUCC) database [72] was used as the main source of high resolution land use and land cover information. This vector dataset was derived from 505 Landsat TM scenes acquired in 2000 that were classified with an overall accuracy of 81% for all of China. Compared to other coarser land cover products such as the IGBP DISCover or GLC2000, the CAS LUCC database has a finer spatial resolution and is more accurate [81]. The original 25 land cover types of the CAS LUCC database were merged into 8 relevant classes for our study region (Table 1, Figure 1(C)).

Table 1. Reclassified Chinese Academy of Sciences (CAS) land cover scheme.

Land Cover Types	Description
Sparse grassland (SG)	Herbaceous land with 5-20% canopy cover
Medium dense grassland (MG)	Herbaceous land with 20-60% canopy cover
Dense grassland (DG)	Herbaceous land with over 60% canopy cover
Croplands (CL)	Agricultural land with crops
Forestland (FL)	Coniferous, broadleaf and mixed tree cover
Waterbodies (WB)	Ocean, lakes, reservoirs, and rivers
Constructed area (CA)	Artificial surfaces
Non-vegetated land (NL)	All other land cover with less than 5% vegetation cover

3. Methods

We used the relatively short time series of MODIS-Terra NDVI between 2001 and 2010 to better understand how well this time series correlates with the SPOT VGT derived NDVI over time. The idea behind this benchmarking was to test how well spatio-temporal patterns can be reproduced between state-of-the-art NDVI archives. If patterns are similar, we can conclude that those are not arbitrary and we can rely on the underlying time series. In a second step we evaluated how AVHRR-GIMMS differs against this benchmark. Comparing AVHRR GIMMS to SPOT VGT data allowed us to take advantage of the maximum temporal overlap between both archives from 1999 to 2006. We first smoothed all the NDVI products by time series fitting and then extracted phenological parameters, NDVI amplitude and integral, from each NDVI time series. We then performed a correlation analysis to investigate the relationship between different NDVI archives. Lastly, we compared NDVI trends based on NDVI values and also based on phenological parameters using non-parametric statistics.

3.1. Time Series Fitting and Phenological Metrics

Several approaches have been developed to eliminate noise in NDVI time series caused by clouds, ozone, dust, as well as off-nadir viewing and low sun zenith angles [82–85]. Most widely used techniques include Best Index Slope Extraction (BISE), Fourier based filtering, Savitzky-Golay and asymmetric Gaussian filters. These techniques are based on a temporal approach, which provides an

estimate of NDVI noise through temporal interpolation [86]. Here, the double logistic function fitting provided in the TIMESAT software was chosen to smooth NDVI time series because of its proven general applicability and superiority to many other filters [84,87]. Pixels flagged as no data (value = −1), snow/ice covered (value = 2) or cloud contaminated (value = 3) in the MOD13Q1 pixel reliability layer were excluded prior to the temporal interpolation. Outliers were identified by a Seasonal-Trend decomposition based on Loess (STL) [83], which is global in character and not dependent on ancillary data [84,88].

Based on the fitted time series, we computed land surface phenological parameters for the AVHRR GIMMS, SPOT-VGT and MODIS Terra NDVI archives. Two frequently used phenological metrics based on NDVI time series, NDVI seasonal amplitude and integral, were derived to analyze both functional and structural dynamics of vegetation. Seasonal amplitude is defined as the difference between the base and maximum NDVI values in each growing cycling. NDVI amplitude indicates the intra-annual dynamics in vegetation phenology and thus has often been used in terrestrial ecosystem classification [35]. The NDVI integral, estimated as the cumulative value of NDVI time series in vegetation growth during the season [89,90], is closely related to net primary productivity. Using TIMESAT, the start of season is defined as 20% of the fitted curve amplitude. We used the so-called "large NDVI integral" defined in TIMESAT [89–91].

3.2. Correlation Analysis

Following [58], we conducted a correlation analysis to test the linear relationship between different NDVI products. In a first step, fitted MODIS Terra NDVI time series data were spatially resampled to meet the coarser resolution of SPOT VGT NDVI time series. Both time series were aggregated to monthly data. MVC and a bilinear interpolation algorithm were used to generate a monthly 1-km MODIS Terra NDVI time series. We then calculated the pixel-wise linear Pearson correlation coefficient (r) between monthly 1-km SPOT VGT and MODIS Terra NDVI values between 2001 and 2010. We compared SPOT VGT and AVHRR GIMMS NDVI time series in a similar fashion. SPOT VGT was aggregated into monthly and 8-km resolution time series for calculating r between SPOT VGT and AVHRR GIMMS NDVI time series.

3.3. Trend Analysis

We calculated linear trends in NDVI time series to analyze patterns of changes and also to test whether a good correlation between NDVI from different global archives can be used to infer a good correlation between trends. We used non-parametric statistical tests, the Modified Seasonal Mann-Kendall (MSK) and Mann-Kendall (M-K) test to evaluate the statistical significance of trends based on (a) all data from monthly fitted NDVI time series and (b) annual values of the NDVI phenological metrics, respectively [92–94]. Unlike ordinary least squares regression, the MSK trend test is less affected by missing values and uneven data distribution, and are robust towards extreme values and serial dependence [85]. To identify the magnitude of a trend, we calculated Sen's slope [95,96] which is a form of robust linear regression and less affected by gross data errors or outliers compared to linear regression analysis [97,98].

The quantitative comparison of trends was conducted based on sampling plots of 8 km × 8 km. To assure homogeneity and minimize the effects of mixed pixels and misregistration, we overlaid the reclassified Landsat-based CAS LUCC database with the sample plots and selected only plots with at least 80% of a single land cover type. Based on that strategy, 2,770 samples were selected for trend analysis, among which 278 plots were labeled as cropland, 199 plots as forestland, 955 plots as dense grassland, 742 plots as medium dense grassland, and 596 as sparse grassland. We then calculated for each sample plot average values of Sen's slope for SPOT VGT, MODIS Terra and AVHRR GIMMS.

4. Results

4.1. Correlation Analysis and Comparing Trends from SPOT VGT and MODIS Terra NDVI Archives

The correlation between NDVI time series from SPOT VGT and MODIS in vegetated areas of Inner Mongolia was larger than 0.9 (Figure 2 (A)). In comparison, NDVI time series showed a correlation less than 0.2 for non-vegetated areas such as the desert in the Alxa Plateau and for water bodies.

Temporal trends derived from SPOT VGT and MODIS time series showed similar spatial patterns (Figure 3). Most areas in Inner Mongolia did not show a significant trend during the past 10 years in neither SPOT VGT nor MODIS data ($p < 0.05$, MSK test). Some regions, however, exhibited significant trends which were also captured in both datasets, e.g., a greening pattern extending from southern Inner Mongolia to the northern Shannxi and Shanxi provinces (Figures 1 and 3). Overall, 0.1% of Inner Mongolia exhibited significant negative and 3.3% significant positive NDVI trends based on SPOT VGT data. MODIS Terra based analyses resulted in 3.4% of the area having a statistically significant vegetation decrease, and 6.0% with a significant increase. Few regions showed trend disagreements ($p < 0.05$, MSK test). Major discrepancies were found in the central Inner Mongolia, where SPOT VGT based trends showed little change and MODIS Terra NDVI decreased. In Hinggan, MODIS Terra NDVI increased less than that from SPOT VGT.

Figure 2. Pearson's correlation coefficient (*r* value) between monthly 1-km Système Probatoire d'Observation de la Terre VEGETATION (SPOT VGT) and Moderate-Resolution Imaging Spectroradiometer (MODIS) (**A**), monthly 8-km SPOT VGT and Advanced Very High Resolution Radiometer Global Inventory Modeling and Mapping Studies (AVHRR GIMMS) (**B**).

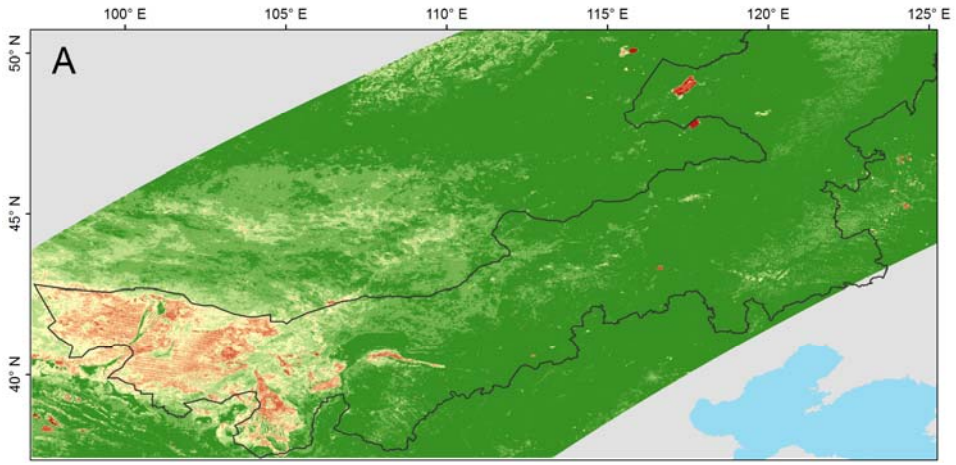

Figure 2. *Cont.*

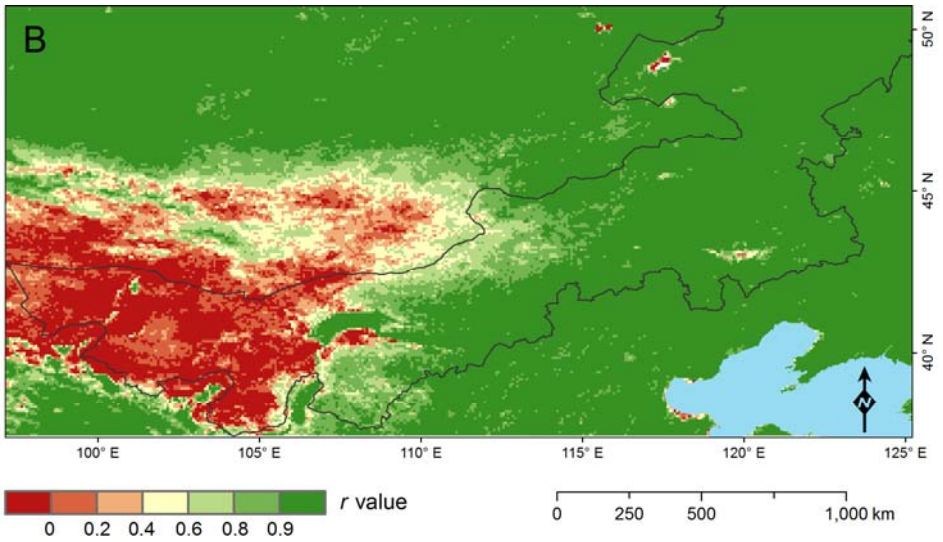

Figure 3. Maps of Normalized Difference Vegetation Index (NDVI) change between 2001 and 2010 based on statistically significant Sen's slope of 1-km SPOT VGT (**A**) and 250-m MODIS (**B**) time series ($p < 0.05$, MSK test). Comparison of Sen's slope values for different phenological parameters based on 2770 sampling plots (**C**).

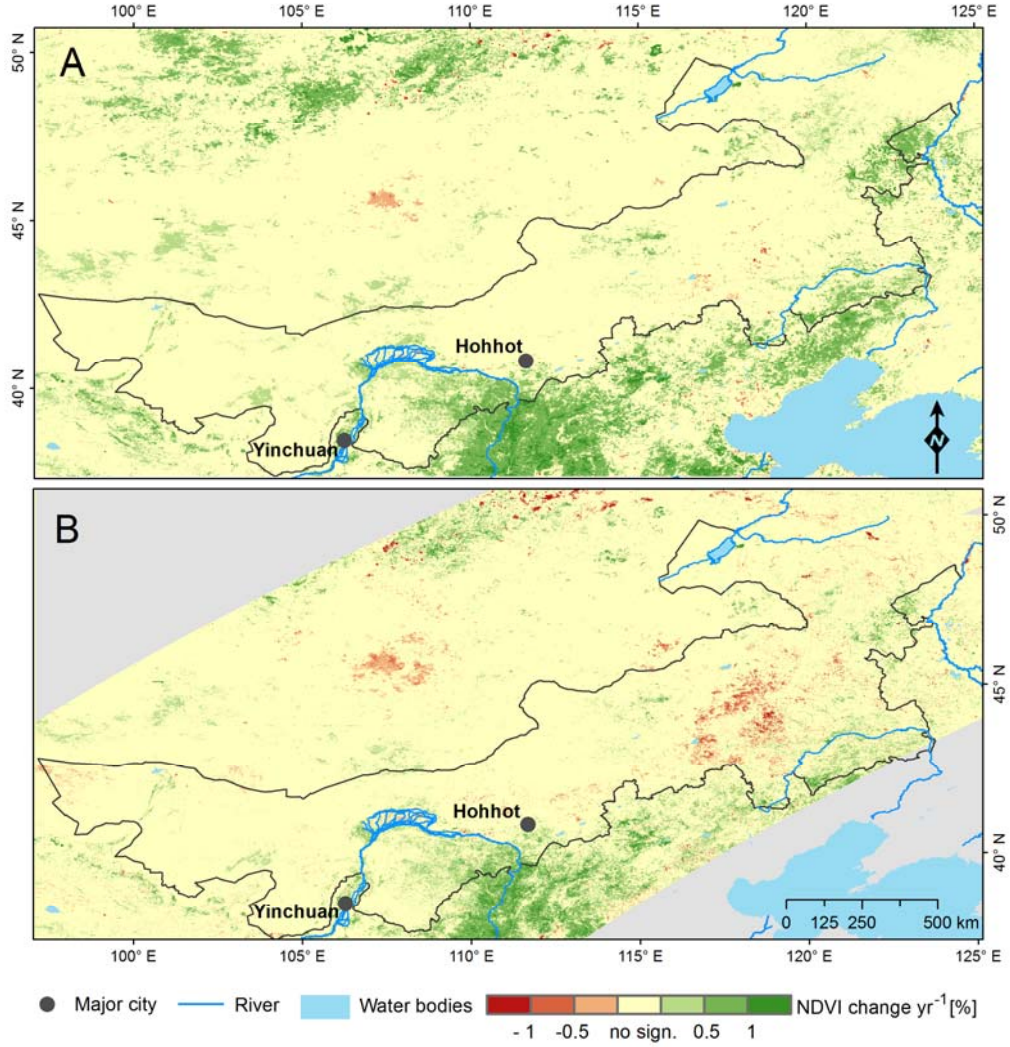

Figure 3. *Cont.*

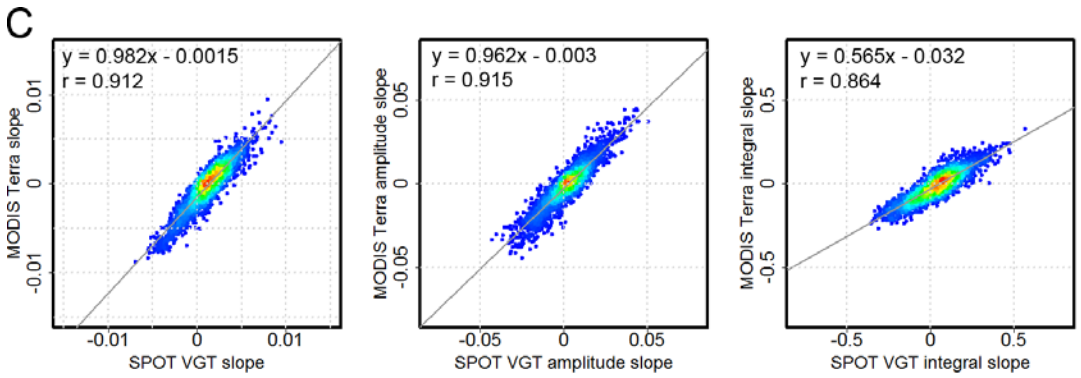

Compared to grassland, croplands showed more widespread increase in NDVI in both NDVI archives (Table 2). About 18.0% and 24.3% of the pixels classified as croplands exhibited a positive trend based on SPOT VGT and MODIS Terra, respectively. Only 0.1% and 1.0% of the cropland pixels were characterized by a decreasing trend in SPOT VGT and MODIS Terra data, respectively. Both NDVI archives showed the smaller NDVI changes for grassland areas. Only 9.8% of the grassland areas showed a significant increase and 0.4% a significant decrease in SPOT VGT data, while based on MODIS Terra 15.4% and 3.9% area of the NDVI in grasslands increased and decreased, respectively.

Table 2. Statistics for SPOT VGT and MODIS Terra NDVI linear trend analysis from 2001 to 2010 ($p < 0.05$, MSK test).

Observation	Cropland Area (%)	Grassland Area (%)
SPOT VGT NDVI positive slope	18.0	9.8
SPOT VGT NDVI negative slope	0.1	0.4
MODIS Terra NDVI positive slope	24.3	15.4
MODIS Terra NDVI negative slope	1.0	3.9

Similarly, we found that the spatial patterns of the trends derived from the NDVI amplitude and integral exhibited high similarities between SPOT VGT and MODIS Terra (not shown here for brevity). The regression analysis between SPOT VGT-derived and MODIS-derived trend parameters further confirmed a good agreement between the two NDVI time series (Figure 3(C)). For example, there was a strong correlation between NDVI trends derived from SPOT VGT and MODIS Terra ($r = 0.91$) time series, and also between trends in NDVI amplitudes ($r = 0.92$). The slope of the fitted regression functions showed a close to a 1:1-relationship. The correlation between Sen's slope of the integral of SPOT VGT against MODIS Terra was lower, but still indicated good correlation ($r = 0.86$). We therefore used the longer SPOT VGT time series for further analyses.

4.2. Correlation Analysis and Comparing Trends from SPOT VGT and AVHRR GIMMS NDVI Archives

The direct comparison between the NDVI time series from SPOT VGT and AVHRR GIMMS showed a similar strong linear correlation between the cyclic vegetation dynamics that dominate both archives. Comparable to the results from our comparison of SPOT VGT and MODIS Terra, NDVI time series from SPOT VGT and AVHRR GIMMS were positively correlated with generally high r values ($r > 0.9$) in vegetated areas of Inner Mongolia (Figure 2(B)).

However, when comparing inter-annual trends between SPOT VGT and AVHRR GIMMS NDVI, major disagreements became apparent (Figure 4(A,B)). Trends from AVHRR GIMMS showed, for example, a significant NDVI decrease in the vegetation-free western part of Inner Mongolia. Almost the whole desert area exhibited this decreasing trend. In comparison, SPOT VGT did not show any significant trends in these areas. Considerable trend disagreement was also evident in northeast Inner Mongolia, where only AVHRR GIMMS-derived trends showed a strong greening pattern. Although the trend patterns from AVHRR GIMMS exhibit similarities with those derived from SPOT VGT in some regions, e.g., greening patterns in southern Inner Mongolia, trend discrepancies clearly prevail at a regional scale. Generally, the substantial trend disagreement in the maps was supported by a low *r* of 0.28, 0.42 and 0.37 (for trends derived from NDVI, amplitude and integral, respectively; Figure 4(C)).

Figure 4. Maps of NDVI change between 1999 and 2006 based on statistically significant Sen's slope of 8-km AVHRR GIMMS (**A**) and 1-km SPOT VGT (**B**) time series ($p < 0.05$, MSK test). Comparison of Sen's slope values for different phenological parameters based on 2,770 sampling plots (**C**).

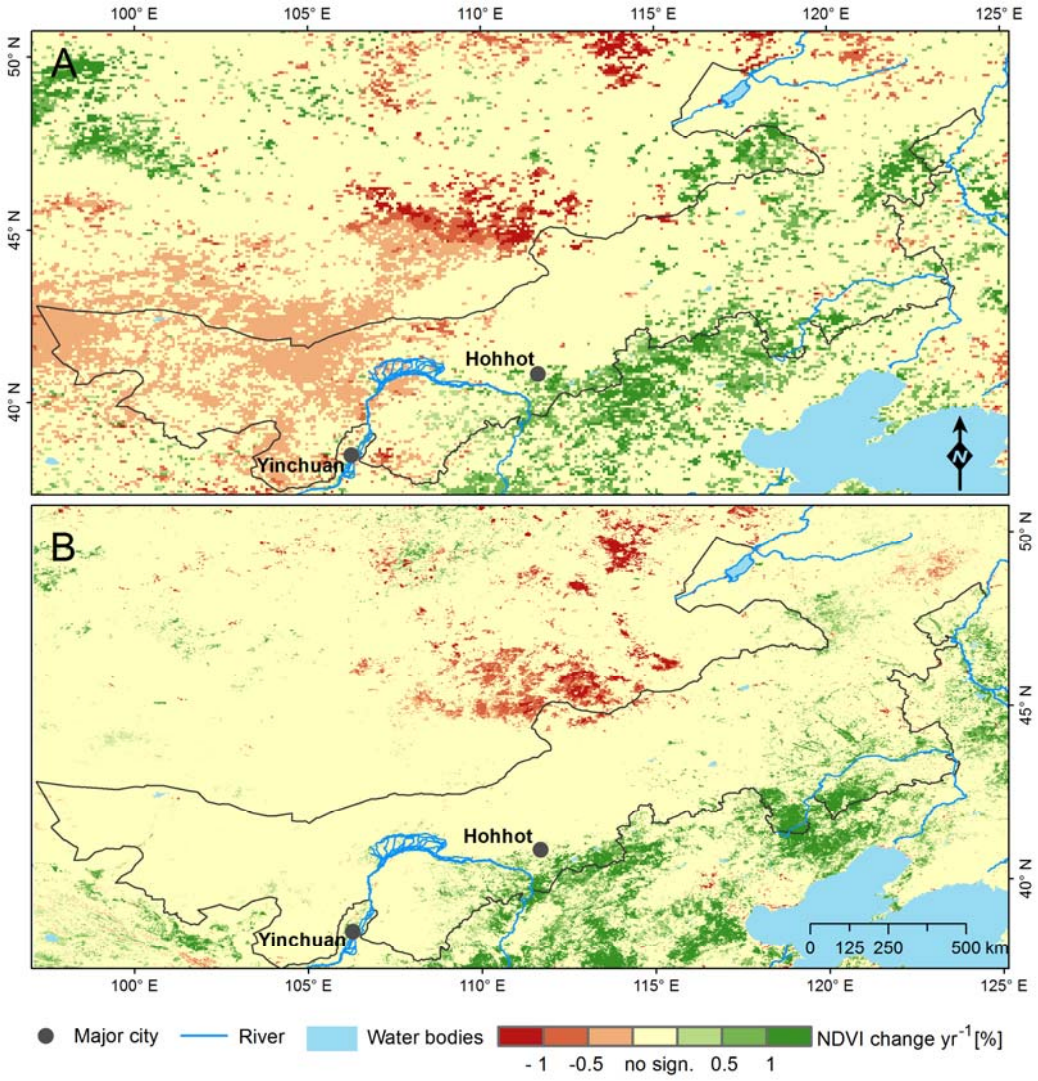

Figure 4. *Cont.*

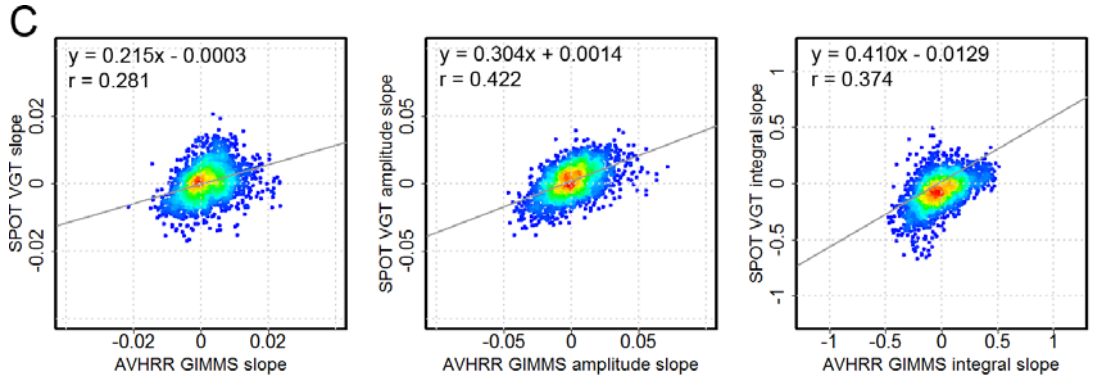

As we were interested in better understanding the causes for the discrepancies, we analyzed if trend differences were associated with specific land cover categories and also if low NDVI values were differently affected than high NDVI values. To answer these questions we first grouped all pixels based on five land cover classes derived from the reclassified CAS map (excluding waterbodies, constructed area, and non-vegetated land), and then we grouped pixels based on 0.1 NDVI intervals from multiannual averages of SPOT VGT NDVI (Figure 5). The slope differences derived from the two archives increased with higher NDVI levels (Figure 5(A)). This was also in agreement with forested areas exhibiting the largest trend disagreement between archives, while sparse grassland correlated better (Figure 5(B)). As grassland fractional cover increased, higher variance in differences and stronger average differences were observed between trends from both archives.

Trends derived from amplitude and integral also support these findings (not shown). Similarly, correlations of AVHRR GIMMS and SPOT VGT-derived Sen's slope values for all phenological parameters were low (Figure 4(C)).

Figure 5. Boxplots of absolute differences between regression (Sen's) slopes derived from SPOT VGT and AVHRR GIMMS time series grouped by land cover types (**A**) and SPOT VGT-based NDVI intervals (**B**). See Table 1 for a description of land cover types. The boxes represent first (25%) and third (75%) quartiles; the whiskers are defined as 1.5 times interquartile. The bold horizontal line in the box represent median.

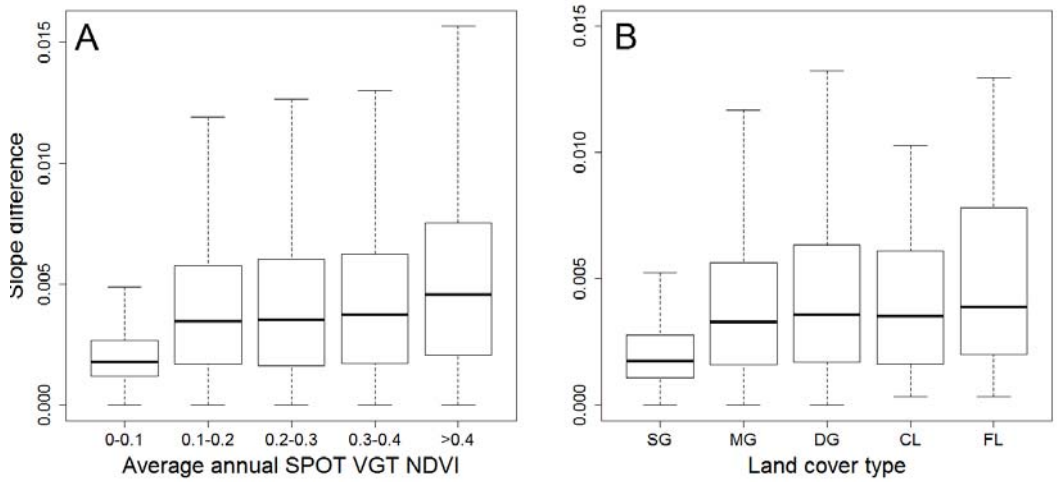

Large trend discrepancies between SPOT VGT and AVHRR GIMMS can be found in our test regions Ordos and Hinggan (Figure 6). Grazing land did generally not exhibit strong trends for the Ordos region (Figure 6(A)), which is reflected in the SPOT VGT derived map. Significant changes between 1999 and 2006 relate to the growing city of Yinchuan and intensified irrigation in its surroundings and along the Yellow River. Quite the opposite, trends from AVHRR GIMMS data clearly suggest strong vegetation cover decreases in the dryland areas, while there is no detection of increased productivity in irrigated west Yinchuan plain. Interestingly, AVHRR GIMMS data estimate changes in the opposite direction for the Hinggan region (Figure 6(B)).

Figure 6. Maps of Sen's slope for AVHRR GIMMS and SPOT VGT from 1999 to 2006 in Ordos (**A**) and Hinggan (**B**). NDVI time series for a sample location in Ordos and Hinggan (below respective maps).

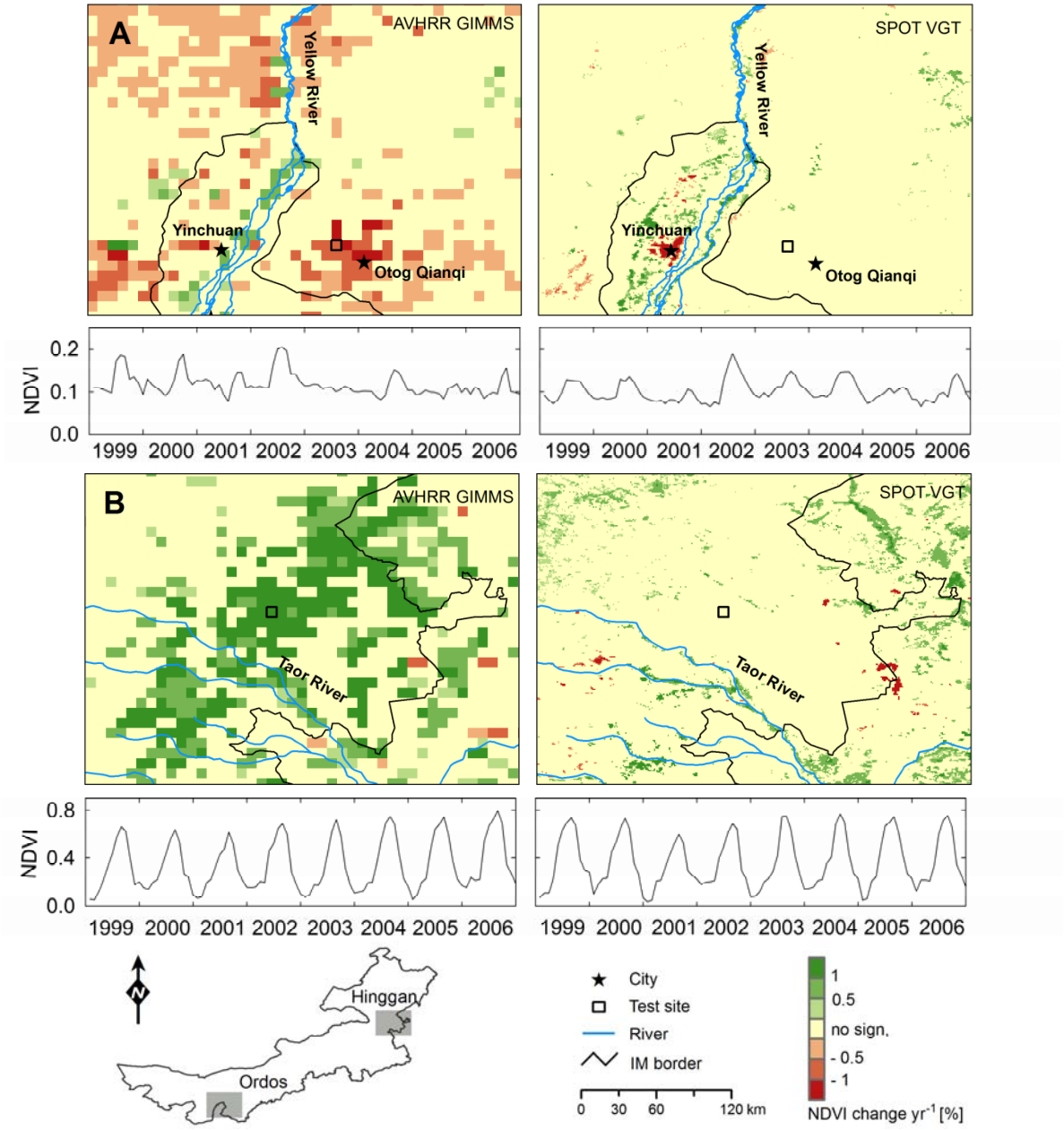

To illustrate the disagreement in NDVI trends from the two archives, we plotted NDVI time series for selected pixels from both focus regions (Figure 6). The samples show that SPOT VGT was able to depict the vegetation seasonality in a semi-arid to arid environment in the Ordos region, while AVHRR GIMMS did not resolve such information in years with low average NDVI (e.g., 2003 and 2005; Figure 6(A)). Major discrepancies also existed in 1999 and 2000 when NDVI values from AVHRR GIMMS were much higher compared to SPOT VGT, leading to a significantly decrease in NDVI for the Ordos region. In the Hinggan region, AVHRR GIMMS deviated from SPOT VGT mostly at the start of the time series (1999 and 2000), while the similarity much improved between these two products for later years. However, the considerably lower values from AVHRR GIMMS NDVI in these two years overall lead to a more positive trend compared to SPOT VGT.

5. Discussion

The high temporal resolution of global data sets such as AVHRR, MODIS and SPOT VGT allows us to derive indicators of agricultural dynamics across the globe. However, spectral mixtures and a broad range of problems largely related to the pre-processing of global remote sensing data sets complicate the interpretation of trends from such coarse resolution data (250 m–8 km). Thus, it is important to gain a deeper knowledge on the reliability of temporal patterns derived from coarse resolution datasets before we interpret trends and link change trajectories to specific agricultural processes.

AVHRR-based NDVI datasets such as the AVHRR GIMMS data constitute the longest hyper-temporal remote sensing records for agricultural monitoring at global scales. Much research related to the impact of global climate change on agricultural productivity and to land degradation monitoring in arid and semi-arid agriculture is based on AVHRR GIMMS [59,91,99–101].

We established a benchmark for analyzing the consistency of AVHRR GIMMS-derived vegetation trends in Inner Mongolia, an important area of agricultural production in China, based on a comparison of MODIS and SPOT-derived trend parameters. Integrating large areas implies that average changes in NDVI are subtle. Still, similar patterns are found when comparing these effects in MODIS and SPOT VGT derived time series. The high consistency between MODIS Terra and SPOT-derived results proves the general reliability of analyses based on these archives. Our comparison shows that different satellite platforms and sensors, differing pre-processing schemes and moderately different spatial resolutions do not hamper the analytical potential of time series analysis when using MODIS Terra and SPOT-derived vegetation products. In Inner Mongolia, analysis based on both MODIS Terra and SPOT VGT allow for successfully analyzing multiple agricultural processes related to a set of agricultural and environmental policies in China addressing increasing agricultural production and decreasing environmental degradation.

Our results from the trend analysis of SPOT VGT and MODIS Terra time series indicate that land degradation processes only marginally affected the agricultural sub-systems of Inner Mongolia during the last decade. Most of Inner Mongolia's grasslands did not exhibit a significant change after the restrictive fencing policies were introduced for all the grassland in Inner Mongolia around the turn of the century. The significantly increasing trend of NDVI in mountainous environment (e.g., Loess Plateau, Yan Mountains) reflects the process of afforestation based on massive subsidization. The "greening" pattern also confirms the effectiveness of China's "Grain for Green" program in Inner

Mongolia in the last decade (Figure 3). However, comparing trends derived from SPOT-VGT and AVHRR GIMMS reveals that major discrepancies can occur when comparing trends from NDVI archives that are more profoundly different. This is also the case when compared the trends from all three NDVI archives during their overlap period (2001–2006) and using increasing kernel size (3 × 3 GIMMS pixels) of sampling plots (not shown for brevity). Differences between NDVI trends seem to increase with increasing NDVI levels (Figure 5(A)). [59] assume on a global level that these deviations relate to land cover classes. Comparing different agricultural land cover categories with trend discrepancies (Figure 5(B)), our findings generally agree with this assumption. From our quantitative analysis across arid to semi-arid biomes, we conclude differently from [58] that the differences in NDVI trends not only affected desert regions but also semi-arid landscapes. However, further tests across a broader range of biomes with in-depth regional information on land use and land cover changes will be needed to quantitatively confirm this finding. Different regional land surface biophysical properties and the limitations of NDVI in relation to the respective sensor characteristics and preprocessing schemes hence contribute to these trend differences [102,103]. Moreover, the sensitivity of trend analysis needs to be tested further to gain a more confident assessment for long-term land degradation [104].

The two focus regions of Ordos and Hinggan served for a more detailed analysis of GIMMS- and SPOT VGT based trends. The Ordos region exhibited a clear decreasing trend in NDVI based on the GIMMS data for the Otog Qianqi grasslands that was not evident from SPOT VGT (Figure 6(A)). Likewise, the GIMMS-based trend analysis did not reflect the immense growth of Yinchuan city (negative trends), which was correctly identified in SPOT VGT-derived trends (Figure 6(A)). Our results for Ordos are in line with findings derived from Landsat data by [105], which indicate a slight vegetation increase across different ecosystems during our observation period. Also, field-based measurements of vegetation cover, height and biomass indicate no broad-scale degradation in the vast grasslands of Otog Qianqi [106]. The patterns related to agricultural intensification along the Yellow River in Ningxia (Figure 1, Figure 6(A)) was captured both by SPOT VGT and AVHRR GIMMS. However, cropland intensification and expansion in the western Yinchuan Plain was not well detected based on AVHRR GIMMS data (Figure 6(A)).

In Hinggan, positive trends were extracted from SPOT VGT data along the Taor River valley. Rice is the main crop along the Taor River, and these positive trends correspond well with the intensified cropping system that was established in the early-1990s [107,108]. AVHRR GIMMS derived trends did clearly not preserve the patterns retrieved from SPOT VGT (Figure 6(B)). While the overall trend is also positive, the greening up for a major area north of the Taor River is largely overestimated, as the intensified irrigation does not prevail across these several 1,000 km^2. Moreover, land use and land cover change assessments based on Landsat data do not support the positive trends identified in AVHRR GIMMS data [64].

We also observed an overall decreasing trend in AVHRR GIMMS-derived NDVI values across non-vegetated areas of Inner Mongolia. This trend was likely caused by satellite drift effects in the signal [109]. NOAA AVHRR platforms do not allow for orbital drift adjustments, resulting in illumination differences affecting NDVI values [110]. According to [73], EMD largely minimizes effects related to orbital drift. However, as AVHRR GIMMS data are not accompanied by metadata on applied pixel-wise EMD correction, it is not possible to conclude on the local effects of EMD.

Further, differences in atmospheric correction algorithms likely contributed to trend discrepancies. Natural variability in column water vapor, ozone and aerosol optical thickness (AOT) in the atmosphere can greatly affect land surface reflectance estimates [111]. Unlike MODIS on the Terra and Aqua platforms, AVHRR does not provide additional spectral channels that allow us to derive information on atmospheric composition to be used for correction [103,112]. To minimize impacts from the atmosphere, a bimonthly MVC is applied for the top-of-atmosphere GAC data to produce AVHRR GIMMS. However, it has been reported that MVC does not significantly improve data quality in regions with persistently high AOT [102,103]. This is most likely the case for Inner Mongolia, where high aerosol loads prevail due to frequent dust storms [113].

Different spatial aggregation algorithms applied for producing NDVI archives certainly contribute to trend discrepancies as well. The input data used for producing the AVHRR GIMMS archive is the GAC 1B product, which is sampled spatially through a combination of line skipping and averaging [114,115]. Each GAC pixel (roughly 3 km by 5 km) is binned into one of the 8 km pixels of the output product based on a forward, nearest neighbor mapping, where the GAC pixel with the highest NDVI value is selected [116]. As a consequence, at least four GAC 1B pixels are mapped to one bin. At nadir, the binning can include up to 6 pixels [116]. The much coarser spatial resolution per AVHRR GIMMS pixel certainly hampers the comparability of AVHRR GIMMS to finer spatial resolution NDVI archives. Specifically, knowledge on the detectability of fine scale processes in 64 km^2 pixels is limited, and statistically valid experiments for increasing our understanding based on field data are complex [117,118]. The small average patch size of Inner Mongolian croplands limits the ability of AVHRR GIMMS for consistent change detection. This is specifically the case for agricultural intensification along the river valley. Taking the smaller absolute vegetation variation in arid and semi-arid environments into account, NDVI derived from AVHRR data are generally less sensitive and hence less correspondent to finer spatial resolution NDVI archives.

Summarizing, our findings indicate a good agreement between trends from SPOT VGT and MODIS Terra for different agricultural land uses across Inner Mongolia, although the spatial and temporal resolution, the spectral bandwidths and preprocessing algorithms are different. This consistency is supported by trends based on phenological indicators derived from original NDVI time series. Overall, trend analyses from AVHRR-related products did in most cases not reproduce similar patterns of change across different agricultural systems across Inner Mongolia.

6. Conclusions

AVHRR GIMMS has regularly been employed for detecting hot-spots of land surface changes via NDVI trend analyses or NDVI-based phenological parameters derived from time series. While comparisons based on the raw time series indicate congruence between AVHRR GIMMS and other NDVI archives, more recent studies based on trend parameters derived from these archives indicate that inconsistencies exist between trends [52,119,120]. We here demonstrated that considerable discrepancies in trend magnitude and direction exist between AVHRR GIMMS and SPOT VGT-based NDVI products (r = 0.28). These discrepancies are exemplified for a range of agricultural land use systems across Inner Mongolia. Analyses based on phenological parameters derived from such NDVI time series lead to comparable dissimilarities (supported by a low r of 0.42 and 0.37 from amplitude

and integral, respectively). While quantifying the magnitude of different factors contributing to these inconsistencies is beyond the scope of this paper (and probably not possible due to the lack of empirical evidence), it is obvious that hyper-temporal NDVI products and related trend analyses from AVHRR GIMMS can strongly differ from those retrieved from instruments such as MODIS Terra and SPOT VGT.

We have shown that such deviations can occur regardless of the chosen trend indicator and across a range of agricultural systems. Comparing significant positive and negative trend hotspots in Ordos and Hinggan derived from SPOT VGT and AVHRR GIMMS revealed that even broad scale changes in vegetation cover can be missed in 8 km AVHRR GIMMS data.

There is an urgent need to better understand the opportunities and limitations of AVHRR GIMMS data in different regions of the world to advise a broad user community on where and how different NDVI archives can be reliably linked to derive longer and more reliable time series. Based on our findings along climate and land-use gradients from the Gobi desert to the northeast of China across the 3,000 km of Inner Mongolia, we caution that monitoring of agricultural lands based on hyper-temporal imagery from AVHRR GIMMS needs to be underpinned with viable consistency checks on the comparability of trends derived from time series in the respective regional setting. We conclude that AVHRR GIMMS and NDVI products from other sensors cannot be combined into homogeneous, long-term time series across the globe without regional sensitivity analyses.

Acknowledgments

This work was supported by the China Scholarship Council (CSC), Grant 2009601084. We want to thank Sebastian van der Linden for helpful comments on the manuscript. We are grateful to Zhengguo Li from the Chinese Academy of Agricultural Sciences (CAAS). We also thank Xueyong Zhao, Hao Qu, and Jie Lian of the Chinese Academy of Sciences (CAS) for their support on field data.

References

1. Millenium Ecosystem Assessment. What are the Most Important Uncertainties Hindering Decision-Making Concerning Ecosystems? In *Ecosystems and Human Well-Being: Synthesis*; Island Press: Washington DC, USA, 2005; p. 101.
2. Tucker, C.J.; Townshend, J.R.G.; Goff, T.E. African land-cover classification using satellite data. *Science* **1985**, *227*, 369–375.
3. Turner, B.L., II; Lambin, E.F.; Reenberg, A. From the cover land change science special feature: The emergence of land change science for global environmental change and sustainability. *Proc. Natl. Acad. Sci.* **2007**, *104*, 20666–20671.
4. Cracknell, A.P. *The Advanced very High Resolution Radiometer (AVHRR)*; Taylor & Francis: London, UK/Bristol, PA, USA, 1997; p. 534.
5. Fensholt, R.; Rasmussen, K.; Nielsen, T.T.; Mbow, C. Evaluation of earth observation based long term vegetation trends—Intercomparing NDVI time series trend analysis consistency of Sahel from AVHRR GIMMS, Terra MODIS and SPOT VGT data. *Remote Sens. Environ.* **2009**, *113*, 1886–1898.

6. Friedl, M.A.; McIver, D.K.; Hodges, J.C.F.; Zhang, X.Y.; Muchoney, D.; Strahler, A.H.; Woodcock, C.E.; Gopal, S.; Schneider, A.; Cooper, A.; *et al.* Global land cover mapping from MODIS: Algorithms and early results. *Remote Sens. Environ.* **2002**, *83*, 287–302.
7. Ganguly, S.; Friedl, M.A.; Tan, B.; Zhang, X.Y.; Verma, M. Land surface phenology from MODIS: Characterization of the collection 5 global land cover dynamics product. *Remote Sens. Environ.* **2010**, *114*, 1805–1816.
8. van Leeuwen, W.J.D.; Huete, A.R.; Laing, T.W. MODIS vegetation index compositing approach: A prototype with AVHRR data. *Remote Sens. Environ.* **1999**, *69*, 264–280.
9. Gutman, G.; Janetos, A.C.; Justice, C.O.; Moran, E.F.; Mustard, J.F.; Rindfuss, R.R.; Skole, D.; Turner, B.L., II; Cochrane, M.A. *Land Change Science: Observing, Monitoring and Understanding Trajectories of Change on the Earth's Surface*; Springer: London, UK, 2004; Volume 1, p. 461.
10. Townshend, J.; Justice, C.; Li, W.; Gurney, C.; McManus, J. Global land cover classification by remote sensing: present capabilities and future possibilities. *Remote Sens. Environ.* **1991**, *35*, 243–255.
11. DeFries, R.S.; Hansen, M.C.; Townshend, J.R.G.; Janetos, A.C.; Loveland, T.R. A new global 1 km dataset of percentage tree cover derived from remote sensing. *Global Change Biol.* **2000**, *6*, 247–254.
12. Barnosky, A.D.; Hadly, E.A.; Bascompte, J.; Berlow, E.L.; Brown, J.H.; Fortelius, M.; Getz, W.M.; Harte, J.; Hastings, A.; Marquet, P.A., *et al.* Approaching a state shift in Earth's biosphere. *Nature* **2012**, *486*, 52–58.
13. Matson, P.A.; Parton, W.J.; Power, A.G.; Swift, M.J. Agricultural intensification and ecosystem properties. *Science* **1997**, *277*, 504–509.
14. Rasmussen, P.E.; Goulding, K.W.T.; Brown, J.R.; Grace, P.R.; Janzen, H.H.; Korschens, M. Long-term agroecosystem experiments: Assessing agricultural sustainability and global change. *Science* **1998**, *282*, 893–896.
15. de Jong, R.; Verbesselt, J.; Schaepman, M.E.; de Bruin, S. Trend changes in global greening and browning: Contribution of short-term trends to longer-term change. *Global Change Biol.* **2012**, *18*, 642–655.
16. Samanta, A.; Costa, M.H.; Nunes, E.L.; Vieira, S.A.; Xu, L.; Myneni, R.B. Comment on "Drought-Induced Reduction in global terrestrial Net Primary Production from 2000 Through 2009". *Science* **2011**, *333*, 1093.
17. Verbesselt, J.; Hyndman, R.; Newnham, G.; Culvenor, D. Detecting trend and seasonal changes in satellite image time series. *Remote Sens. Environ.* **2010**, *114*, 106–115.
18. Verbesselt, J.; Hyndman, R.; Zeileis, A.; Culvenor, D. Phenological change detection while accounting for abrupt and gradual trends in satellite image time series. *Remote Sens. Environ.* **2010**, *114*, 2970–2980.
19. Reed, B.C.; Brown, J.F. Trend Analysis of Time-Series Phenology Derived from Satellite Data. In *Proceedings of 2005 International Workshop on the Analysis of Multi-Temporal Remote Sensing Images*, Biloxi, MI, USA, 16–18 May 2005; pp. 166–168.
20. Tucker, C.J.; Dregne, H.E.; Newcomb, W.W. Expansion and contraction of the Sahara Desert from 1980 to 1990. *Science* **1991**, *253*, 299–301.

21. Udelhoven, T.; Stellmes, M.; Del Barrio, G.; Hill, J. Assessment of rainfall and NDVI anomalies in Spain (1989–1999) using distributed lag models. *Int. J. Remote Sens.* **2009**, *30*, 1961–1976.
22. Myneni, R.B.; Keeling, C.D.; Tucker, C.J.; Asrar, G.; Nemani, R.R. Increased plant growth in the northern high latitudes from 1981 to 1991. *Nature* **1997**, *386*, 698–702.
23. Pettorelli, N.; Vik, J.O.; Mysterud, A.; Gaillard, J.M.; Tucker, C.J.; Stenseth, N.C. Using the satellite-derived NDVI to assess ecological responses to environmental change. *Trends Ecol. Evol.* **2005**, *20*, 503–510.
24. Tucker, C.J. Red and photographic infrared linear combinations for monitoring vegetation. *Remote Sens. Environ.* **1979**, *8*, 127–150.
25. Field, C.B.; Behrenfeld, M.J.; Randerson, J.T.; Falkowski, P. Primary production of the biosphere: Integrating terrestrial and oceanic components. *Science* **1998**, *281*, 237–240.
26. Panda, S.S.; Ames, D.P.; Panigrahi, S. Application of vegetation indices for agricultural crop yield prediction using neural network techniques. *Remote Sens.* **2010**, *2*, 673–696.
27. Labus, M.P.; Nielsen, G.A.; Lawrence, R.L.; Engel, R.; Long, D.S. Wheat yield estimates using multi-temporal NDVI satellite imagery. *Int. J. Remote Sens.* **2002**, *23*, 4169–4180.
28. Boschetti, M.; Stroppiana, D.; Brivio, P.A.; Bocchi, S. Multi-year monitoring of rice crop phenology through time series analysis of MODIS images. *Int. J. Remote Sens.* **2009**, *30*, 4643–4662.
29. de Beurs, K.M.; Henebry, G.M. Land surface phenology, climatic variation, and institutional change: Analyzing agricultural land cover change in Kazakhstan. *Remote Sens. Environ.* **2004**, *89*, 497–509.
30. Hill, M.J.; Donald, G.E. Estimating spatio-temporal patterns of agricultural productivity in fragmented landscapes using AVHRR NDVI time series. *Remote Sens. Environ.* **2003**, *84*, 367–384.
31. Lee, R.; Yu, F.; Price, K.P.; Ellis, J.; Shi, P. Evaluating vegetation phenological patterns in Inner Mongolia using NDVI time-series analysis. *Int. J. Remote Sens.* **2002**, *23*, 2505–2512.
32. Xin, J.; Yu, Z.; van Leeuwen, L.; Driessen, P.M. Mapping crop key phenological stages in the North China Plain using NOAA time series images. *Int. J. Appl. Earth Obs.* **2002**, *4*, 109–117.
33. Kariyeva, J.; Van Leeuwen, W. Environmental drivers of NDVI-based vegetation phenology in Central Asia. *Remote Sens.* **2011**, *3*, 203–246.
34. Reed, B.C.; White, M.; Brown, J.F. Remote Sensing Phenology. In *Phenology: An Integrative Environmental Science*; Schwartz, M.D., Ed.; Kluwer Academic Publishers: Dordrecht, The Netherlands, 2003; pp. 365–380.
35. Bradley, B.A.; Mustard, J.F. Comparison of phenology trends by land cover class: A case study in the Great Basin, USA. *Global Change Biol.* **2008**, *14*, 334–346.
36. Yu, H.Y.; Luedeling, E.; Xu, J.C. Winter and spring warming result in delayed spring phenology on the Tibetan Plateau. *Proc. Natl. Acad. Sci.* **2010**, *107*, 22151–22156.
37. Alcantara, C.; Kuemmerle, T.; Prishchepov, A.V.; Radeloff, V.C. Mapping abandoned agriculture with multi-temporal MODIS satellite data. *Remote Sens. Environ.* **2012**, *124*, 334–347.
38. Gu, Y.; Brown, J.; Miura, T.; Van Leeuwen, W.J.; Reed, B. Phenological classification of the United States: A geographic framework for extending multi-sensor time-series data. *Remote Sens.* **2010**, *2*, 526–544.

39. Martinez-Beltran, C.; Jochum, M.A.O.; Calera, A.; Melia, J. Multisensor comparison of NDVI for a semi-arid environment in Spain. *Int. J. Remote Sens.* **2009**, *30*, 1355–1384.
40. Zhang, X.Y.; Friedl, M.A.; Schaaf, C.B.; Strahler, A.H.; Hodges, J.C.F.; Gao, F.; Reed, B.C.; Huete, A. Monitoring vegetation phenology using MODIS. *Remote Sens. Environ.* **2003**, *84*, 471–475.
41. Geerken, R.; Ilaiwi, M. Assessment of rangeland degradation and development of a strategy for rehabilitation. *Remote Sens. Environ.* **2004**, *90*, 490–504.
42. Li, A.; Deng, W.; Liang, S.; Huang, C. Investigation on the patterns of global vegetation change using a satellite-sensed vegetation index. *Remote Sens.* **2010**, *2*, 1530–1548.
43. Wessels, K.J.; Prince, S.D.; Malherbe, J.; Small, J.; Frost, P.E.; VanZyl, D. Can human-induced land degradation be distinguished from the effects of rainfall variability? A case study in South Africa. *J. Arid Environ.* **2007**, *68*, 271–297.
44. Begue, A.; Vintrou, E.; Ruelland, D.; Claden, M.; Dessay, N. Can a 25-year trend in Soudano-Sahelian vegetation dynamics be interpreted in terms of land use change? A remote sensing approach. *Global Environ. Change* **2011**, *21*, 413–420.
45. Lillesand, T.M.; Kiefer, R.W.; Chipman, J.W. *Remote Sensing and Image Interpretation*, 6th ed.; John Wiley & Sons: Hoboken, NJ, USA, 2008; p. 768.
46. Steven, M.D.; Malthus, T.J.; Baret, F.; Xu, H.; Chopping, M.J. Intercalibration of vegetation indices from different sensor systems. *Remote Sens. Environ.* **2003**, *88*, 412–422.
47. Huete, A.; Didan, K.; Miura, T.; Rodriguez, E.P.; Gao, X.; Ferreira, L.G. Overview of the radiometric and biophysical performance of the MODIS vegetation indices. *Remote Sens. Environ.* **2002**, *83*, 195–213.
48. Tarnavsky, E.; Garrigues, S.; Brown, M.E. Multiscale geostatistical analysis of AVHRR, SPOT-VGT, and MODIS global NDVI products. *Remote Sens. Environ.* **2008**, *112*, 535–549.
49. Jiang, H. Grassland management and views of nature in China since 1949: Regional policies and local changes in Uxin Ju, inner Mongolia. *Geoforum* **2005**, *36*, 641–653.
50. Li, W.J.; Ali, S.H.; Zhang, Q. Property rights and grassland degradation: A study of the Xilingol Pasture, Inner Mongolia, China. *J. Environ. Manage.* **2007**, *85*, 461–470.
51. Tucker, C.J.; Pinzon, J.E.; Brown, M.E.; Slayback, D.A.; Pak, E.W.; Mahoney, R.; Vermote, E.F.; El Saleous, N. An extended AVHRR 8-km NDVI dataset compatible with MODIS and SPOT vegetation NDVI data. *Int. J. Remote Sens.* **2005**, *26*, 4485–4498.
52. Alcaraz-Segura, D.; Liras, E.; Tabik, S.; Paruelo, J.; Cabello, J. Evaluating the consistency of the 1982–1999 NDVI trends in the Iberian Peninsula across four time-series derived from the AVHRR sensor: LTDR, GIMMS, FASIR, and PAL-II. *Sensors* **2010**, *10*, 1291–1314.
53. Brown, M.E.; Pinzon, J.E.; Didan, K.; Morisette, J.T.; Tucker, C.J. Evaluation of the consistency of long-term NDVI time series derived from AVHRR, SPOT-Vegetation, SeaWiFS, MODIS, and Landsat ETM+ sensors. *IEEE Trans. Geosci. Remote Sens.* **2006**, *44*, 1787–1793.
54. Gitelson, A.A.; Kaufman, Y.J. MODIS NDVI optimization to fit the AVHRR data series spectral considerations. *Remote Sens. Environ.* **1998**, *66*, 343–350.
55. Fontana, F.; Rixen, C.; Jonas, T.; Aberegg, G.; Wunderle, S. Alpine grassland phenology as seen in AVHRR, VEGETATION, and MODIS NDVI time series—A comparison with *in situ* measurements. *Sensors* **2008**, *8*, 2833–2853.

56. Gallo, K.; Li, L.; Reed, B.; Eidenshink, J.; Dwyer, J. Multi-platform comparisons of MODIS and AVHRR normalized difference vegetation index data. *Remote Sens. Environ.* **2005**, *99*, 221–231.
57. Swinnen, E.; Veroustraete, F. Extending the SPOT-VEGETATION NDVI time series (1998–2006) back in time with NOAA-AVHRR data (1985–1998) for southern Africa. *IEEE Trans. Geosci. Remote Sens.***2008**, *46*, 558–572.
58. Song, Y.; Ma, M.G.; Veroustraete, F. Comparison and conversion of AVHRR GIMMS and SPOT vegetation NDVI data in China. *Int. J. Remote Sens.* **2010**, *31*, 2377–2392.
59. Fensholt, R.; Proud, S.R. Evaluation of Earth observation based global long term vegetation trends—Comparing GIMMS and MODIS global NDVI time series. *Remote Sens. Environ.* **2012**, *119*, 131–147.
60. Yu, F.F.; Price, K.P.; Ellis, J.; Shi, P.J. Response of seasonal vegetation development to climatic variations in eastern Central Asia. *Remote Sens. Environ.* **2003**, *87*, 42–54.
61. Nemani, R.R.; Keeling, C.D.; Hashimoto, H.; Jolly, W.M.; Piper, S.C.; Tucker, C.J.; Myneni, R.B.; Running, S.W. Climate-driven increases in global terrestrial net primary production from 1982 to 1999. *Science* **2003**, *300*, 1560–1563.
62. Tao, F.L.; Yokozawa, M.; Zhang, Z.; Xu, Y.L.; Hayashi, Y. Remote sensing of crop production in China by production efficiency models: Models comparisons, estimates and uncertainties. *Ecol. Model.* **2005**, *183*, 385–396.
63. Liu, J.Y.; Liu, M.L.; Zhuang, D.F.; Zhang, Z.X.; Deng, X.Z. Study on spatial pattern of land-use change in China during 1995–2000. *Sci. China Ser. D* **2003**, *46*, 373–384.
64. Liu, J.Y.; Zhang, Z.X.; Xu, X.L.; Kuang, W.H.; Zhou, W.C.; Zhang, S.W.; Li, R.D.; Yan, C.Z.; Yu, D.S.; Wu, S.X.; Nan, J. Spatial patterns and driving forces of land use change in China during the early 21st century. *J. Geogr. Sci.* **2010**, *20*, 483–494.
65. Wang, X.H.; Lu, C.H.; Fang, J.F.; Shen, Y.C. Implications for development of grain-for-green policy based on cropland suitability evaluation in desertification-affected North China. *Land Use Policy* **2007**, *24*, 417–424.
66. Jiang, H. Decentralization, ecological construction, and the environment in post-reform China: Case study from Uxin Banner, Inner Mongolia. *World Development* **2006**, *34*, 1907–1921.
67. Tong, C.; Wu, J.; Yong, S.; Yang, J.; Yong, W. A landscape-scale assessment of steppe degradation in the Xilin River Basin, Inner Mongolia, China. *J. Arid Environ.* **2004**, *59*, 133–149.
68. Chen, J.S.; He, D.W.; Cui, S.B. The response of river water quality and quantity to the development of irrigated agriculture in the last 4 decades in the Yellow River Basin, China. *Water Resour. Res.* **2003**, *39*, 1047.
69. Qiao, G.H.; Zhao, L.J.; Klein, K.K. Water user associations in Inner Mongolia: Factors that influence farmers to join. *Agr. Water Manage.* **2009**, *96*, 822–830.
70. Bennett, M.T. China's sloping land conversion program: Institutional innovation or business as usual? *Ecol. Econ.* **2008**, *65*, 699–711.
71. Deng, X.Z.; Huang, J.K.; Rozelle, S.; Uchida, E. Cultivated land conversion and potential agricultural productivity in China. *Land Use Policy* **2006**, *23*, 372–384.
72. Liu, J.; Liu, M.; Deng, X.; Zhuang, D.; Zhang, Z.; Luo, D. The Land-use and land-cover change database and its relative studies in China. *J. Geogr. Sci* **2002**, *12*, 275–282.

73. Pinzon, J.E.; Brown, M.E.; Tucker, C.J. Monitoring Seasonal and Interannual Variations in Land-Surface Vegetation from 1981–2006 Using GIMMS NDVI. University of Maryland-Global Land Cover Facility Data Distribution. Available online: http://glcf.umiacs.umd.edu/library/guide/GIMMSdocumentation_NDVIg_GLCF.pdf (accessed on 30 July 2007).
74. Pinzon, J. Using HHT to Successfully Uncouple Seasonal and Interannual Components in Remotely Sensed Data. In *Proceedings of SCI 2002 International Conference*, Orlando, FL, USA, 14–18 July 2002.
75. Pinzon, J.; Brown, M.E.; Tucker, C.J. Satellite Time Series Correction of Orbital Drift Artifacts Using Empirical Mode Decomposition. In *Hilbert-Huang Transform: Introduction and Applications*; Huang, N.E., Shen, S.P., Eds.; World Scientific Publishing Company: Hackensack, NJ, USA, 2004.
76. Mangiarotti, S.; Mazzega, P.; Hiernaux, P.; Mougin, E. The vegetation cycle in West Africa from AVHRR-NDVI data: Horizons of predictability *versus* spatial scales. *Remote Sens. Environ.* **2010**, *114*, 2036–2047.
77. Gobron, N.; Pinty, B.; Verstraete, M.M.; Widlowski, J.L. Advanced vegetation indices optimized for up-coming sensors: Design, performance, and applications. *IEEE Trans. Geosci. Remote Sens.* **2000**, *38*, 2489–2505.
78. *SPOT Vegetation User's Guide*. Available online: http://www.spot-vegetation.com/userguide/userguide.htm (assessed on 1 June 2011).
79. Henry, P.; Meygret, A. Calibration of Vegetation Cameras on-board SPOT4. In *Proceedings of 2000 Conference on the VEGETATION*, Belgirate, Italy, 3–6 April 2001; pp. 23–32.
80. Vermote, E.F.; El Saleous, N.Z.; Justice, C.O. Atmospheric correction of MODIS data in the visible to middle infrared: First results. *Remote Sens. Environ.* **2002**, *83*, 97–111.
81. Ran, Y.H.; Li, X.; Lu, L. China land cover classification at 1 km spatial resolution based on a multi-source data fusion approach. *Adv. Earth Sci.* **2009**, *24*, 192–203.
82. Gutman, G.; Ignatov, A. Satellite-derived green vegetation fraction for the use in numerical weather prediction models. *Adv. Space Res.* **1997**, *19*, 477–480.
83. Holben, B.N. Characteristics of maximum-value composite images from temporal AVHRR data. *Int. J. Remote Sens.* **1986**, *7*, 1417–1434.
84. Jonsson, P.; Eklundh, L. TIMESAT—A program for analyzing time-series of satellite sensor data. *Comput. Geosci.* **2004**, *30*, 833–845.
85. Udelhoven, T. TimeStats: A software tool for the retrieval of temporal patterns from global satellite archives. *IEEE J. Sel. Top. Appl. Earth Obs. Remote Sens.* **2011**, *4*, 310–317.
86. Julien, Y.; Sobrino, J.A. Comparison of cloud-reconstruction methods for time series of composite NDVI data. *Remote Sens. Environ.* **2010**, *114*, 618–625.
87. Hird, J.N.; McDermid, G.J. Noise reduction of NDVI time series: An empirical comparison of selected techniques. *Remote Sens. Environ.* **2009**, *113*, 248–258.
88. Cleverland, R.B.; Cleveland, W.S.; McRae, J.E. A seasonal-trend decomposition procedure based on Loess. *J. Official Stat.* **1990**, *6*, 3–73.
89. Jonsson, P.; Eklundh, L. Seasonality extraction by function fitting to time-series of satellite sensor data. *IEEE Trans. Geosci. Remote Sens.* **2002**, *40*, 1824–1832.

90. White, M.A.; de Beurs, K.M.; Didan, K.; Inouye, D.W.; Richardson, A.D.; Jensen, O.P.; O'Keefe, J.; Zhang, G.; Nemani, R.R.; van Leeuwen, W.J.D.; *et al.* Intercomparison, interpretation, and assessment of spring phenology in North America estimated from remote sensing for 1982–2006. *Global Change Biol.* **2009**, *15*, 2335–2359.
91. Heumann, B.W.; Seaquist, J.W.; Eklundh, L.; Jonsson, P. AVHRR derived phenological change in the Sahel and Soudan, Africa, 1982–2005. *Remote Sens. Environ.* **2007**, *108*, 385–392.
92. Hirsch, R.M.; Slack, J.R. A Nonparametric trend test for seasonal data with serial dependence. *Water Resour. Res.* **1984**, *20*, 727–732.
93. Kendall, M.G. *Rank Correlation Methods*, 4 ed.; Charles Griffin: London, UK, 1975; p. 202.
94. Mann, H.B. Non-parametric test against trend. *Econometrica* **1945**, *13*, 245–259.
95. Hirsch, R.M.; Slack, J.R.; Smith, R.A. Techniques of trend analysis for monthly water-quality data. *Water Resour. Res.* **1982**, *18*, 107–121.
96. Sen, P.K. Estimates of regression coefficient based on Kendall's Tau. *J. Am. Stat. Assoc.* **1968**, *63*, 1379–1389.
97. Bouza-Deano, R.; Ternero-Rodriguez, M.; Fernandez-Espinosa, A.J. Trend study and assessment of surface water quality in the Ebro River (Spain). *J. Hydrol.* **2008**, *361*, 227–239.
98. Gilbert, R.O. *Statistical Methods for Environmental Pollution Monitoring*; Van Nostrand Reinhold Company: New York, NY, USA, 1987; p. 320.
99. Dent, D.L.; Bai, Z.G.; Olsson, L.; Schaepman, M.E. Proxy global assessment of land degradation. *Soil Use Manage.* **2008**, *24*, 223–234.
100. Helldén, U.; Tottrup, C. Regional desertification: A global synthesis. *Global Planet. Change* **2008**, *64*, 169–176.
101. Symeonakis, E.; Drake, N. Monitoring desertification and land degradation over Sub-Saharan Africa. *Int. J. Remote Sens.* **2004**, *25*, 573–592.
102. Kobayashi, H.; Dye, D.G. Atmospheric conditions for monitoring the long-terrn vegetation dynamics in the Amazon using normalized difference vegetation index. *Remote Sens. Environ.* **2005**, *97*, 519–525.
103. Nagol, J.R.; Vermote, E.F.; Prince, S.D. Effects of atmospheric variation on AVHRR NDVI data. *Remote Sens. Environ.* **2009**, *113*, 392–397.
104. Wessels, K.J.; van den Bergh, F.; Scholes, R.J. Limits to detectability of land degradation by trend analysis of vegetation index data. *Remote Sens. Environ.* **2012**, *125*, 10–22.
105. Zhu, Z.H.; Yin, X.R.; Zang, H.B.; Liu, H.M.; Dong, J.L.; Liu, Q.Q.; Li, J.R.; Ruan, X.P. Dynamic monitoring on forestry resources in Etuoke Qianqi based on the interpretation of TM image. *Inner Mongolia Forestry Science & Technology* **2008**, *34*, 45–48.
106. Hasbagen. The Dynamic Studies on Grassland Vegetation Types and Characteristic in Etuokeqian Banner. Thesis of Master, Inner Mongolia Agricultural University: Huhhot, Inner Mongolia, China, 2009.
107. Liu, Q.; He, Y.; Cui, B.S. Land use/cover change and its influence on the evapotranspiration in Taoer River basin. *Resour. Sci.* **2007**, *29*, 121–126.
108. Xia, B.C.; Hu, J.M. Analysis of land-use change in taoerhe catchment during last 15 years. *J. Soil Water Conserv.* **2004**, *11*, 5–8.

109. Deng, M.; Di, L. Solar Zenith Angle Correction of Global NDVI Time-Series from AVHRR. In *Proceedings of IEEE 2001 International Geoscience and Remote Sensing Symposium*, Sydney, NSW, Australia, 9–13 July 2001; Volume 4, pp. 1838–1840.
110. Sobrino, J.A.; Julien, Y.; Atitar, M.; Nerry, F. NOAA-AVHRR orbital drift correction from solar zenithal angle data. *IEEE Trans. Geosci. Remote Sens.* **2008**, *46*, 4014–4019.
111. Kaufman, Y.J. Atmospheric effect on spectral signature—Measurements and corrections. *IEEE Trans. Geosci. Remote Sens.* **1988**, *26*, 441–450.
112. King, M.D.; Kaufman, Y.J.; Menzel, W.P.; Tanre, D. Remote-sensing of cloud, aerosol, and water-vapor properties from the Moderate Resolution Imaging Spectrometer (MODIS). *IEEE Trans. Geosci. Remote Sens.* **1992**, *30*, 2–27.
113. Wang, J.; Xia, X.G.; Wang, P.C.; Christopher, S.A. Diurnal variability of dust aerosol optical thickness and Angstrom exponent over dust source regions in China. *Geophys. Res. Lett.* **2004**, *31*, L08107.
114. Goward, S.N.; Dye, D.G.; Turner, S.; Yang, J. Objective assessment of the NOAA global vegetation index data product. *Int. J. Remote Sens.* **1993**, *14*, 3365–3394.
115. POES (US); NCDC (US). *Technical Documentation with Imagery and Digital Data: NOAA Polar Orbiter Data User's Guide (August 1997) and NOAA Global Vegetation Index User's Guide (July 1997)*, 1.0 ed.; National Climatic Data Center: Asheville, NC, USA, 1997.
116. James, M.E.; Kalluri, S.N.V. The pathfinder AVHRR land data set—An improved coarse resolution data set for terrestrial monitoring. *Int. J. Remote Sens.* **1994**, *15*, 3347–3363.
117. Gupta, R.K.; Prasad, T.S.; Rao, P.V.K.; Manikavelu, P.M.B. Problems in upscaling of high resolution remote sensing data to coarse spatial resolution over land surface. *Adv. Space Res.* **2000**, *26*, 1111–1121.
118. Hufkens, K.; Bogaert, J.; Dong, Q.H.; Lu, L.; Huang, C.L.; Ma, M.G.; Che, T.; Li, X.; Veroustraete, F.; Ceulemans, R. Impacts and uncertainties of upscaling of remote-sensing data validation for a semi-arid woodland. *J. Arid Environ.* **2008**, *72*, 1490–1505.
119. Baldi, G.; Nosetto, M.D.; Aragon, R.; Aversa, F.; Paruelo, J.M.; Jobbagy, E.G. Long-term satellite NDVI data sets: Evaluating their ability to detect ecosystem functional changes in South America. *Sensors* **2008**, *8*, 5397–5425.
120. Beck, H.E.; McVicar, T.R.; van Dijk, A.I.J.M.; Schellekens, J.; de Jeu, R.A.M.; Bruijnzeel, L.A. Global evaluation of four AVHRR-NDVI data sets: Intercomparison and assessment against Landsat imagery. *Remote Sens. Environ.* **2011**, *115*, 2547–2563.